Splicing variants of versican in CD133$^+$/CD44$^+$ prostate cancer stem cells

Sule Ayla [a,*], Emre Karakoc [b], Yasemin Yozgat Byrne [c], Cuneyd Parlayan [d], Ilknur Keskin [c,e], Sercin Karahuseyinoglu [f], Aysegul Taskiran [g], Gulperi Oktem [g]

[a] Istanbul Medeniyet University, School of Medicine, Department of Histology and Embryology, Istanbul 34700, Turkey
[b] Wellcome Sanger Institute, Cambridge, England, United Kingdom
[c] Research Institute for Health Sciences and Technologies (SABITA), Cancer Research Center, Istanbul Medipol University, Beykoz, Istanbul 34810, Turkey
[d] Bahçeşehir University School of Medicine, Department of Biostatistics and Medical Informatics, Sahrayıcedit, Istanbul 34353, Turkey
[e] Istanbul Medipol University, School of Medicine, Department of Histology and Embryology, Istanbul 34810, Turkey
[f] Koc University, School of Medicine, Department of Histology and Embryology, Sariyer, Istanbul 34450, Turkey
[g] Ege University, School of Medicine, Department of Histology and Embryology, Bornova, Izmir 35100, Turkey

ARTICLE INFO

ABSTRACT

A cancer mass is composed of a heterogeneous group of cells, a small part of which constitutes the cancer stem cells since they are less differentiated and have a high capacity to develop cancer. Versican is an extracellular matrix protein located in many human tissues. The mRNA of versican has been shown to have "splicing patterns" as detected by RT-PCR, northern blot analysis, and cDNA sequencing. Based on this knowledge this study aims to reveal the splice variants of versican molecules, which are thought to be involved in the pathogenesis of the DU-145 human prostatic carcinoma cell line and prostatic cancer stem cells isolated from this cell line. In this study, RWPE-1 normal prostatic and DU-145 human prostate cancer cell lines have been used. Prostatic cancer stem cells and the remaining group of non-prostatic-cancer stem cells (bulk population) were isolated according to their CD133$^+$/CD44$^+$. RNA was isolated in all groups, and sequence analysis was accomplished for splicing variants by Illumina NextSeq 500 sequencing system. The results were analyzed by bioinformatic evaluation. As five isoforms of the versican gene in the differential transcript expression are analyzed, it was observed that a significant change was only found in the isoforms Versican 0 and Versican 1. In this study, we explored the function of this molecule which we think to be effective in cancer progression, and suggested that more valuable results can be obtained after the accomplishment of in vivo experiments.

1. Introduction

Prostate cancer is a common tumor in men [1]. Many reasons increase the risk of prostate cancer (for example, family factors, gonorrhea, and smoking) [2,3], and genetic predisposition is considered to be one of the important factors in the incidence of prostate cancer [1,4].

Cancer is the clonal expansion of cells with defective growth mechanisms, and it can be considered the most common and complicated form of somatic genetic disease [5]. Cancer is now largely understood to be a disease impacted by the tumor microenvironment, rather than just a cell and gene expression issue. Tumor development, progression, and metastasis are facilitated by interactions between immune cells, fibroblasts, extracellular matrix, and signaling chemicals, which are constituents of the tumor microenvironment [6]. The main structure of this environment is composed of the parenchymal and stromal growth factors, leukocytes, chemokines, inflammatory mediators, and matrix metalloproteinase enzymes. Cancer cells and cancer stem cells (CSCs) form a heterogeneous community in the parenchyma, while the stroma contains an extracellular matrix. Cancers are composed of heterogeneous cell populations exhibiting different biological properties and tumorigenic potential. Among these cell populations, only the mixture of stem cells and proliferative cells can regenerate a tumor through the

stem cell processes of self-renewal and differentiation into all cell types within the specific tumor [7].

CSCs are cancer cells that carry characteristics alike to normal stem cells. CSCs are identified in many cancer types, including hematological and solid tumors. CSCs can be identified in different ways in several solid malignancies, including clonogenicity, differentiation capacity, the ability of spheroid formation, expression of stemness-related genes, and the ability to produce the original tumor upon transplantation in immunodeficient mice [8].

In cancer, the extracellular matrix (ECM) is a fundamental component of the tumor microenvironment, and it plays an important role in providing cell-adhesion sites. Additionally, being a reservoir for growth factors, ECM is critical for tissue homeostasis [9]. ECM is a dynamic three-dimensional network of extracellular molecules that provide structural and biochemical support to surrounding cells. This structure is composed of a variety of proteins, glycoproteins, proteoglycans, and polysaccharides that possess different biochemical properties and the major components are collagen, fibrin, fibronectin, proteoglycan, and hyaluronan [10,11]. Proteoglycans, compose the central part of the ECM and provide structure, viscosity, lubrication, and adhesiveness [12]. When the extracellular matrix is destroyed, the tumor gains the ability to invade and metastasize.

Versican (VN), a key ingredient of the extracellular matrix, is a chondroitin sulfate proteoglycan. VN and its 4 splice variants (isoform) are localized in the ECM and are all associated with the other ECM components involved in biological activities such as cell adhesion, migration, and proliferation [13,14]. Studies that have been conducted, have shown that VN has an important role in the regulation of the cell phenotype [15,16]. VN expression is associated with the proliferative cell phenotype and is frequently found in highly proliferative tumor types as well as tissues such as the breast [17–19], brain [20], prostate [21,22], and melanoma [23,24] during development. Furthermore, VN expression levels in the prostate stroma are positively correlated with progression in early prostate cancer [21,25]. In vitro studies have shown that VN plays a vital role in cell adhesion [26], aggregation [27], migration [28], cell proliferation [29], morphogenesis [30], and tissue angiogenesis [28]. Although high VN expression is correlated with cancer progression, no study shows the role of VN splice variants in prostate cancer progression.

In our study, we aimed to determine the possible role of splice variants of VN in the pathogenesis of prostate cancer stem cells. Determination of splice variants and their differential expression levels compared to that of normal prostate cells is essential for understanding the pathogenesis of cancer.

2. Materials & methods

2.1. Cell lines and cell culture conditions

Human prostate cancer cell line DU-145 and normal prostate cell line RWPE-1 were purchased from the American Type Culture Collection (ATCC; Rockville, MD, USA). RPMI-1640 medium (Biological Industries) was used for the growing and maintenance of the DU-145 human prostate cancer cell line. For 500 ml sterile medium, 1 % penicillin/streptomycin, 10 % fetal bovine serum (heat inactivated), 1 % amphotericin B, and 1 % L-glutamine is added. Keratinocyte serum-free medium (Invitrogen, 17005-075) supplemented with L-glutamine, epithelial growth factor, and bovine pituitary extract was used to grow and maintain the RWPE-1 human normal prostate epithelial cell line. All cells were grown at 37°C, with 5 % CO$_2$ in a humified incubator. Cell lines were monitored daily in terms of viability, proliferation, and contamination by an inverted microscope. Cells were passaged when more than 80 % cell density was observed in the flasks.

2.2. Fluorescence-activated cell sorting and experimental groups

DU-145 human prostate cancer cells were grown in RPMI-1640 (Lonza, BE12–167 F) medium supplemented with 1 % L-Glutamine (Thermo Scientific, SH3003401), 10 % FBS (Biowest, S1810), 1 % Amphotericin B (Lonza, 17–836E) and 1 % Penicillin/Streptomycin (Thermo Scientific, SV30010), on 75 cm^2 sterile polystyrene cell culture flasks (Corning). Later the cells were treated with 0.05 % Trypsin-EDTA (Lonza) for 5 min at (37°C, with 5 % CO$_2$) to detach off the flask surface. Following trypsin inactivation, the mixture is centrifuged at 1000 rpm for 5 min (Thermo SL 16 R). The supernatant was discarded, as the pellet was resuspended in PBS. 10 µl of this sample is used for cell counting after staining with trypan blue (Sigma Biotechnology, USA). The remaining cells were centrifugated twice for 5 min at 300 rpm. The supernatant was removed, and cells were incubated with CD44-FITC (Clone B-F24, GenProbe USA) and CD133-PE (Miltenyi Biotech, UK) for 20 min at room temperature in the dark. The prostate CSCs expressing CD133$^+$/CD44$^+$ surface markers and the remaining (non-sorting) cells were separated into two tubes by fluorescence-activated cell separation (FACS) method using a flow cytometry analyzer device (BD influx cell sorter, USA). CD133$^+$/CD44$^+$ cells were collected in 5 ml tubes that contained 2 ml of RPMI-1640 medium. To verify the stemness characteristics, the spheroid-forming potential of prostate CSCs isolated by FACS was assessed as reported by Tatar and her colleagues [31]. These cells were then seeded onto 25 cm^2 sterile polystyrene cell culture flasks (Corning) for replication. Four experimental groups were formed following the sorting and replication of the cells:

Group 1: RWPE-1 control cells (normal prostate cell line)
Group 2: DU-145 prostate cancer cell line
Group 3: DU-145 CD133$^+$/CD44$^+$ CSCs (prostate cancer stem cells) (sorted)
Group 4: DU-145 remaining cells after removal of CD133$^+$/CD44$^+$; non-CSCs (non-sorted)

2.3. Gene analysis

RNA isolations from 4 groups of cell types were synthesized into cDNA and quantified using RT-PCR. These cDNAs were then sequenced using the Illumina NextSeq 500 to a desirable coverage. The sequencing data were analyzed in order to understand the gene expression and the variations in the Versican gene and its isoforms. Computational methods for gene expression quantification and differential gene expression were performed during the analysis of the RNA-Seq data.

RNA isolation. RNA isolation was performed by RNeasy Plus Mini Kit (Qiagen, Lot No: 148050825) as recommended by the manufacturer. Briefly, lysis and homogenized cells were isolated from genomic DNA, and 75 ng/µl total RNA was isolated. The RNA quality was measured using UV absorbance unit spectra Max i3 (Molecular Devices).

Library preparation. Library preparation and sequencing were performed with TruSeq Stranded RNA LT kit (Illumina, Ref: 15032612, Lot: 10037008). Briefly, 750 ng total RNA was first fragmented (isolated) with RiboZero (Illumina Lot: 10035196), and cDNA synthesis was performed in two steps (Illumina, Lot: 10035192). After the Polyadenylation of the three prime terminals, the RNA fragments were attached to the adapters. The fragments that were later attached to the adapters are PCR amplified as the kit recommends. The samples were pooled and normalized by mixing with 10 nM Tris-HCI and Tween-20.

Library quantitation. The library was quantitated with the Kappa library quantification (Illumina, Lot: KK4824) method using a real-time PCR device (CFX Connect, BioRad). The libraries are loaded to the PCR machine at 20 pM with 10 µl reaction volume. The melting curves and average Cq score = 7.20 were determined as the quality criteria. The values that are below the required quality were eliminated.

RNA Sequencing. Triple replicas of the groups were sequenced using Nextseq500 (Illumina) for 18 h. The clustering quality of the reads with a minimum of 300 base pair fragments is checked using the CTE1, CTE2,

CTA, and CTL controls that are recommended by Illumina.

2.4. Bioinformatics analysis and quality control

The raw data generated by NextSeq 500 was transformed into short sequencing reads in Fastq format from 4 libraries from each sample using the Bioscape (Illumina) program. The short reads that were obtained from each sample were evaluated together using the quality values of the reads via the FASTQC program (Germany). Before proceeding with the analysis of the data, the reads were controlled for the quality values of the reads, the total number of the reads, and the lengths of each library. During our analysis of the RNA-Seq data, there were not significantly differentially expressed genes between the DU-145 prostate cancer cell line and the sorted non-stem cell prostate cancer tissue. As a result, in this study among the four groups of cells, three groups were focused on; Group 1: control RWPE-1 (normal prostate cell line), Group 2: DU-145 CD133$^+$/CD44$^+$ CSCs (prostate cancer stem cells), Group 3: non-CSCs (prostate cancer non-stem cell group). Three replicates were sequenced to provide the necessary statistical power when performing differential gene expression analyses that compare different cell types.

2.5. Quantification of gene expressions

Following the quality control of the short high throughput RNA-Seq, reads are mapped to the human reference sequence hg38 to quantify the expression of the genes in the human genome. The number of the reads that are mapped to the genes that are normalized by the library size and the gene size is used for quantifying the expression of these genes. The STAR method was used for performing the read alignment. The STAR method is sensitive to the alignment of the reads that span the exon-exon junctions where the reads are split and mapped to their appropriate exons. The STAR alignment is performed in two phases. In phase 1, the reads are mapped to the reference using the gene annotations from Ensembl hg38.89 (in GFT form), and the reads that are not mapped to the reference are split and mapped to the reference genome. In the second phase, the novel junctions and the reference annotation are merged, and this merged novel annotation is used for mapping the RNA-Seq reads. In the RNA-Seq methods, the primary assumption is that the number of reads that are mapped to a gene is proportional to the expression of this gene. Before normalizing and quantifying the gene expression levels, the number of reads that are mapped to all genes in the genome was counted. The counting of the aligned reads is performed using the htseq-count program. These counts are then used for the differential gene expression analysis.

2.6. Differential gene expressions (statistical analysis)

The expression of the genes is quantified (described in the previous section) as the read counts. In order to identify the outliers and the clustering of the replicates, Principal Component Analysis (PCA) was applied. Using the clustering of the different components of the PCA analysis, the quality and the consistency of the RNA-Seq experiments were checked. The differential gene expression analysis was performed using the DESeq2 (v1.18). DESeq2 uses the read counts for identifying the differential gene expression. The read counts were normalized using the Variance Stabilized Normalization method in the DESeq2 package. The variation of the gene expression with the same mean values is assumed to be similar and fit to match a negative binomial distribution. Based on the estimated distribution, the variation is adjusted. The resulting normalized counts are tested for significantly differential expression between groups using the Wald statistical test implemented in the DESeq2 package. To ensure statistical power, three replicates for every group were assessed. For each gene, the p-values were calculated, and these values were corrected for the multiple sample testing using the Benjamini-Hochberg method. After the correction, the genes that were differentially expressed between the two groups that were being tested

were determined using the false discovery rate (FDR) cut-off of 0.05. All the genes that have a corrected p-value below 0.05 were selected as differentially expressed genes.

2.7. Transcript level differential gene expression analysis

The previous analysis estimated the gene expression as reading counts per gene. However, for the transcript analysis, the expression of each isoform that is annotated for each gene was estimated. To perform the transcript-level expression, the Kallisto (v 0.43.1) method was used. The reads were pseudo-mapped to the reference transcriptome instead of the reference genome. Based on the pseudo-mappings, Kallisto estimated the transcript level expression per gene by an expectation-maximization (EM) method. This program was performed with standard parameters with v100 bootstraps and hg38 human reference GTF v89 was used as a reference transcript. The obtained isoform gene expression data were analyzed with the Sleuth (v0.29.0) program, which is specifically developed to be used with the Kallisto program. The differential gene expression was performed using a likelihood ratio test. The main difference between sleuth compared to the other methods is that sleuth uses a variance decomposition model that aims to differentiate the noise variance and the biological variance. The significance of each transcript/isoform was calculated as well as the FDR. The p-value corresponding to the False Discovery Rate (FDR) of 0.05 was calculated over this distribution and significant differentially expressing isoforms are detected using this p-value.

2.8. Quantitative real-time PCR (qRT-PCR) validation of versican isoform expression

Total RNA was extracted with TRIzol reagent (Invitrogen) (10^7 cells per milliliter) (Ambion, Austin, TX) and the RNA purity was assessed by Thermo NanoDrop 2000 (Thermo Fisher Scientific, Inc.) by standard absorbance ratios as A260/A280 $\geq$1.8 and A260/A230 $\geq$1.5. Complementary DNAs were synthesized from 2 μg of total RNA using the RevertAid First Strand cDNA Synthesis Kit (Thermo Fisher Scientific, Inc.). Any potential non-specific amplification of genomic DNA with non-template and no reverse transcription (no-RT) control was applied. qRT-PCR quantification of VN mRNA isoforms using SYBR Green Master chemistry with the SensiFAST™ SYBR No-ROX Kit (Bio Line, London, U. K.) on an iCycler Real-Time Quantitative PCR System (Bio-Rad, Hercules, CA) was performed according to the manufacturer's protocol. The housekeeping gene GAPDH was included as an internal control. The reactions were repeated in triplicate and the resultant mean threshold cycles were used for further analysis. The thermal protocol was as follows: 95°C for 2 min, 45 cycles of denaturation at 95°C for 5 s, annealing at 59°C for 10 s, and elongation with optics on for fluorescence monitoring at 72°C for 10 s, and Melt Curve 65°C to 95°C: Increment 0.5°C 0:05. The threshold cycle (Ct) for individual reactions was identified using iCycler IQ sequence analysis software (Bio-Rad). Versican isoforms: V0 and V1 expression data were normalized to GAPDH as an internal control, and relative gene expressions were presented with the $2-\Delta\Delta Ct$ method [32,33]. The following primers used in this study were purchased from Sentromer DNA Technology Service, Ltd. (Istanbul, Turkey) with the following sequences:

V0: forward 5′-GGTCAGAGAAAATAAGACAGGTCG-3′ and reverse 5′-TCCTTGGGCACAGTGGTAAC-3′

V1: forward 5′-ACTGCTTTAAACGTCGAATGAGTG-3′ and reverse 5′-TCCTTGGGCACAGTGGTAAC-3′

GAPDH: forward 5′-TCCTGCACCACCAACTG-3′ and reverse 5′-TCTGGGTGGCAGTGATG-3′.

3. Results

3.1. Differential gene analysis of prostate cancer tissue cell types

The expressions of the genes in control cells (RWPE-1, normal prostate cell line), DU-145 CD133$^+$/CD44$^+$ CSCs, and DU-145 non-CSCs that are not stem cells are plotted as PCA components after the normalization of the counts using the DESeq2 (v1.18). When we inspected the PCA plots, we observed that the cell types are clustering according to their group types which reassured us that the cell types are differentiated between each other and have some underlying biological reasons for this separation. To understand the differences in the biological activities between these cell types, the differential gene expression between these cell groups was investigated to detect any significant increase or decrease in gene expression between two different cell types. Two differential gene expression analyses were performed: (i) between control (RWPE-1) and CSCs (DU-145 CD133$^+$/CD44$^+$ CSCs) and (ii) between control (RWPE-1) and non-CSCs groups.

3.2. Comparison of control and CSCs groups

As the gene annotation from ensemble human reference gene annotation v89 was explored, seven isoforms for the versican gene were identified. Among these seven isoforms, only five of them were detected to be protein-coding. These protein-coding isoforms of the versican gene were identified as follows:

ENST00000265077.7 VN0 (Versican 0)
ENST00000343200.9 VN1 (Versican 1)
ENST00000342785.8 VN2 (Versican 2)
ENST00000502527.2 VN3 (Versican 3)
ENST00000512590.6 VN4 (Versican 4

The differential gene expression among these groups was calculated using the estimated transcript abundances from the pseudo-alignment of the high throughput next-generation short-read sequencing (RNA-Seq) to the reference transcriptome via the Kallisto (v 0.43.1) method. The clustering of the CSCs group and the RWPE-1 normal human prostate epithelial cell group in the PCA plots has demonstrated that our estimates of the transcripts have been meaningful and the differential expression analysis between these groups can detect the biological processes that are different between these groups (Fig. 1). As five isoforms of the versican gene in the differential transcript expression are analyzed, it was observed that a significant change was only found in the isoforms VN0 and VN1 (Table 1). Compared to the control group, a significant reduction of the transcript expression was observed in cancer stem cells in the following two isoforms: VN0 ($p < 0.05$) and VN1 ($p < 0.001$) (Fig. 2).

3.3. Comparison of control and non-CSCs

Similar to the previous section the clustering of experimental groups was investigated via the use of use PCA plot. It has been detected that the groups are clustering correctly, and the differential transcript expression
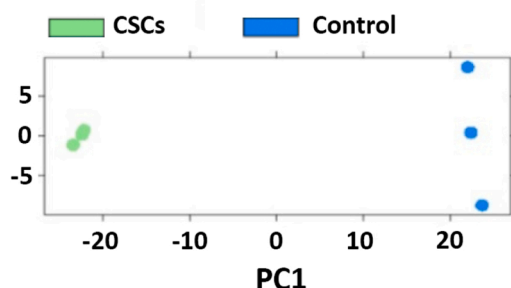
analysis can be performed to uncover the differences between these groups (Fig. 3). According to the results of differential transcriptome analysis, a significant reduction was observed in VN0 ($p < 0.05$) and VN1 ($p < 0.001$) isoforms (Table 2) (Fig. 4).

3.4. Comparison of CSCs and non-CSCs

In our clustering analysis comparing the groups using the PCA plot, we found that the groups were clustering correctly and that the differential transcript analysis between these groups can be performed (Fig. 5). According to the results of transcriptome analysis performed between the groups, it was observed that only VN0 isoform expression was significantly reduced ($p < 0.05$) (Table 3) (Fig. 6).

3.5. Quantitative real-time PCR (qRT-PCR) analysis

According to the qRT-PCR analysis in which the gene expression profile of RWPE-1 normal prostate epithelial cells was used as the reference group, expression of VN0 is decreased in CSCs ($p < 0.05$), non-CSCs ($p < 0.01$) and DU-145 prostate cancer cell line ($p < 0.001$). Similarly based on the qRT-PCR results, VN1 expression is decreased in CSCs ($p < 0.01$), non-CSCs ($p < 0.001$), and DU-145 prostate cancer cell line ($p < 0.001$) (Fig. 7).

4. Discussion

The present study intends to identify the isoforms of VN that are effective in DU-145 prostate cancer stem cells and non-cancer stem cell groups, and to verify the hypothesis related to the presence of a different molecular structure in addition to known variants. Although in several studies, the central role of the expression of versican in tumor cells has been underlined, the role of the host stromal versican is still not well understood. In a recent study, it has been reported that cancer-related fibroblast-related molecules, including VN, are expressed in the stroma of esophageal squamous cell carcinoma and are associated with poor relapse-free and overall survival of patients [34]. Targeting the stromal expression of VN and such molecules may be a potential therapeutic strategy for improving the prognosis of cancer patients [35]. In our study, a statistically significant differential transcript expression was observed only for VN0 and VN1 within the five isoforms of VN, as depicted by the results of the gene expression analysis of RWPE-1, DU-145 prostate CSCs and non-CSCs groups. Increased expression of VN0 and VN1 isoforms in different tumors suggests that this differential expression pattern may be related to tumor development [36]. The results obtained in this study have revealed that VN0 and VN1, which are the main VN isoforms, are active in vitro, especially in prostate CSCs and non-CSCs. There was no evidence of changes in the expression levels of the other isoforms in these cell groups. When the expression of VN isoforms was determined by specifically designed primers, it was observed that the expression levels of VN0 and VN1 isoforms were significantly decreased compared to that of normal prostate epithelial cell lines. It is also claimed that the VN expression levels vary in different tumor cell lines [37–39]. Many previous in vitro studies have focused on VN expression in only tumor cells, however, a comparison regarding the expression profile in normal prostate epithelial cells has not been accomplished. Differences regarding the stromal VN expressions in different tumor cells are still being investigated by several study groups [40–44].

VN expression in pancreatic neuroendocrine tumors has been linked to tumor grade, stage, and patient survival, indicating that it may be useful as a prognostic indicator [45]. VN is linked to the proliferation, invasion, and migration of tumors and is increased in gastric cancer. VN expression is significantly correlated with Tregs, indicating that it may be involved in immune regulation. For gastric cancer patients, VN may be a target for cancer therapy as well as a possible prognostic predictor [46,47]. VN was indicated as a putative PT marker by microproteomics

Fig. 1. Principal component analysis of CSCs and control cells.

Table 1

Differential gene expression analyses of control cells and CSCs.

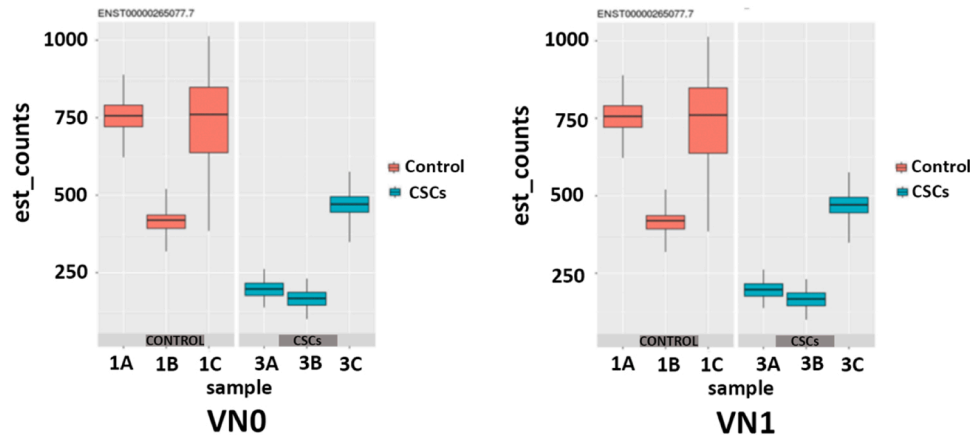| Transcript_id	Isoform	test_stat	P-val	mean_obs	var_obs
ENST00000265077.7	VN0	5,004193	0,025286	5,9725	0,42803
ENST00000343200.9	VN1	8,7017	0,003179	6,03634	1,01733
ENST00000342785.8	VN2	not significant			
ENST00000502527.2	VN3	not significant			
ENST00000512590.6	VN4	not significant			

Fig. 2. The comparative analysis of VN0 and VN1 transcripts in control cells and CSCs.
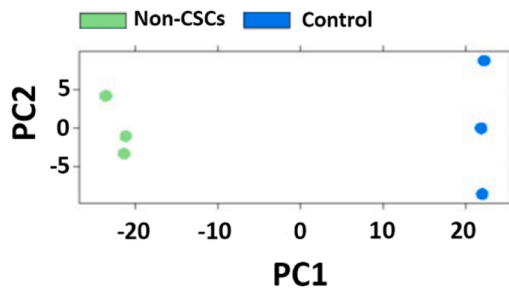

Fig. 3. Principal component analysis of non-CSCs and control cells.

analysis and confirmed its function in phyllodes tumor grading. The grade of phyllodes tumors was shown to be correlated with VN expression, indicating that this protein may be used as a diagnostic and prognostic marker for these tumors [48]. In a study, VN was chosen as a research focus after RNA sequencing showed that the most differentially expressed genes in the upper urinary tract urothelial carcinoma were involved in extracellular matrix structure. In vitro analysis revealed that VN knockdown decreased cell migration. In addition, the efficacy of epirubicin, gemcitabine, and cisplatin was enhanced by silencing VN, suggesting possible therapeutic applications [49]. Suhovskih et al. investigated the expressions of different proteoglycans (versican, decorin, lumican, and syndecan 1) in tissue samples taken from patients with prostate cancer and benign prostatic hypertrophy. They observed no difference between expression levels of VN in prostate tumors and

normal prostate tissue [50]. In contrast to their results, there are publications that bear data showing elevated levels of VN protein associated with disease progression in early prostate cancer [23,50,51]. These results have been attributed to the reduction of VN degradation in prostate cancer tissue or post-transcriptional activation of VN expression [50]. Contrary to the studies that have been mentioned, our results show that the expression levels of the VN isoforms, VN0 and VN1 in prostate CSCs and non-CSCs were significantly decreased compared to normal prostate epithelial cell lines.

In our previous study [52], CSCs isolated from the DU-145 prostate cancer cell line or from its lineage were compared for the adhesion molecules and the changes in cellular structures in two different cell culture types of monolayer and three-dimensional spheroid cultures. Specific genes have been targeted in the analysis of microarray-based gene expression. TGFβ1 expression level was significantly increased in CSCs monolayer cell cultures, and the VN expression level was significantly increased in CSCs three-dimensional spheroid cultures. The results of immunohistochemistry have also confirmed that there is a significant increase in the immunoreactivity of TGFβ1 in monolayer cell cultures and expression of VN in spheroid cultures [52]. Depending on this data, we thought that CSCs were affected by many signaling pathways in the initiation and differentiation of tumor formation. In this study, we showed that in DU-145 prostate CSCs and non-CSCs grown as two-dimensional cell culture models, VN was present in the form of VN0 and VN1 isoforms and it was also demonstrated that the expression of these isoforms was significantly reduced with respect to normal prostate epithelial cell lines. This result suggests that VN plays an important role in tumor organization, especially when CSCs are transformed from
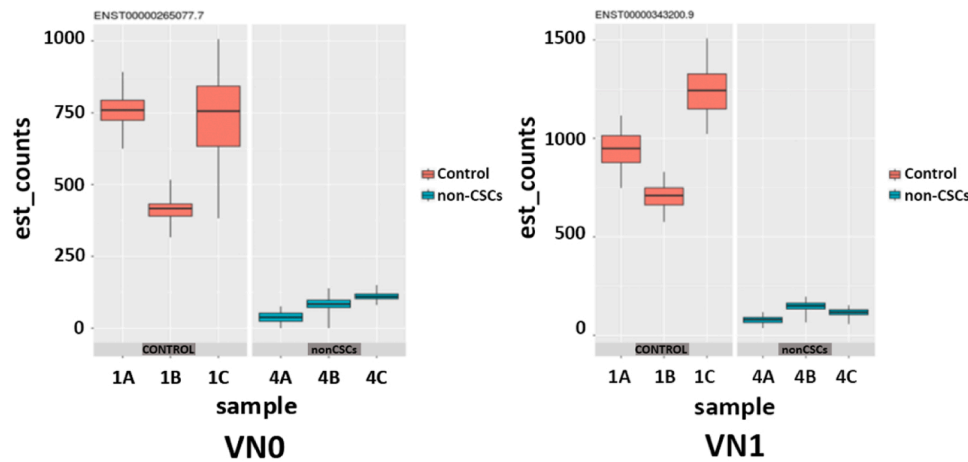
Table 2

Differential gene expression analyses of non-CSCs and control cells.

Transcript_id	Isoform	test_stat	P-val	mean_obs	var_obs
ENST00000265077.7	VN0	9,867461	0,001682275	5,354131	1,568272
ENST00000343200.9	VN1	18,16838	2,02E-05	5,803372	1,36532
ENST00000342785.8	VN2	not significant			
ENST00000502527.2	VN3	not significant			
ENST00000512590.6	VN4	not significant			

Fig. 4. The comparative analysis of VN0 and VN1 transcripts in control cells and non-CSCs.
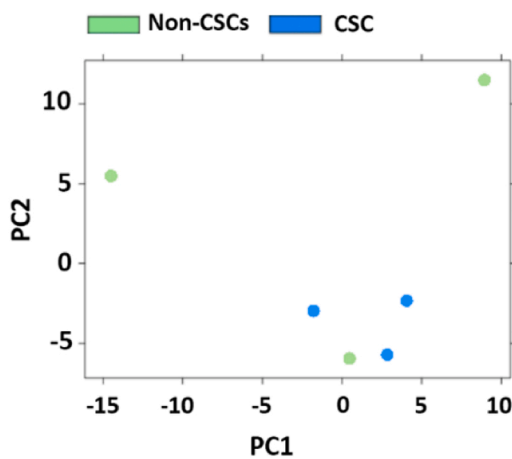

Fig. 5. Principal component analysis of non-CSCs and CSCs.

two-dimensional to three-dimensional structures. Many articles have shown that cancer stem cells which are known to have self-renewal and differentiation capacity, are responsible for the recurrence of the disease at the potential origin of the tumor and chemoresistance [53].

With these results, it is clear that tumor microenvironment and cell heterogeneity play a very important role in tumor growth, progression, and metastasis. When CSCs were organized to arrange into a complex structure as in a spheroid model the VN expression increased, on the other hand, with this study we have shown that the expression of both VN0 and VN1 isoforms decreased in two-dimensional CSCs and non-CSCs. Moreover, the comparison of CSCs and non-CSCs showed that VN0 expression was significantly decreased, suggesting the role of CSCs in tumor organization. To reach a more comprehensive explanation related to tumor organization, in vivo studies should be carried out under the guidance of in vitro studies.

As a result, when we consider cancer as a whole; heterogeneous cancer cells and CSCs are located in the parenchyma, while non-

malignant cells (inflammatory cells, cancer-associated fibroblasts, angiogenic vascular cells, and sometimes adipocytes) and the ECM constitute the stroma. All these substructures that are observed within this complete picture of cancer play a very serious role in the explanation of cancer mechanisms. In this study, which we started with the aim of understanding the role of VN in CSCs and non-CSCs in comparison to normal epithelial cells using two-dimensional cell cultures, we explored the function of this molecule which we think to be effective in cancer progression and suggested that more valuable results can be obtained after the accomplishment of in vivo experiments.

5. Conclusion

Our study delves into the differential expression patterns of VN isoforms in DU-145 prostate CSCs and non-CSCs, shedding light on their potential role in tumor progression. The tumor microenvironment, comprising immune cells, fibroblasts, and extracellular matrix components, plays a pivotal role in cancer development. Our findings reveal a significant decrease in the expression of VN0 and VN1 isoforms in both CSCs and non-CSCs compared to normal prostate epithelial cells. This suggests a nuanced role for VN in tumor organization, especially as CSCs transition from two-dimensional to three-dimensional structures. While in vitro studies highlight the importance of cell heterogeneity and microenvironment interactions, future in vivo investigations will provide a more comprehensive understanding. Overall, our research underscores the intricate involvement of VN isoforms in prostate cancer, emphasizing their potential as therapeutic targets and prognostic indicators. Further exploration in both experimental and clinical settings is warranted to validate and extend these observations.

Ethics approval and consent to participate

Not applicable.

Table 3
Differential gene expression analyses of non-CSCs and CSCs.

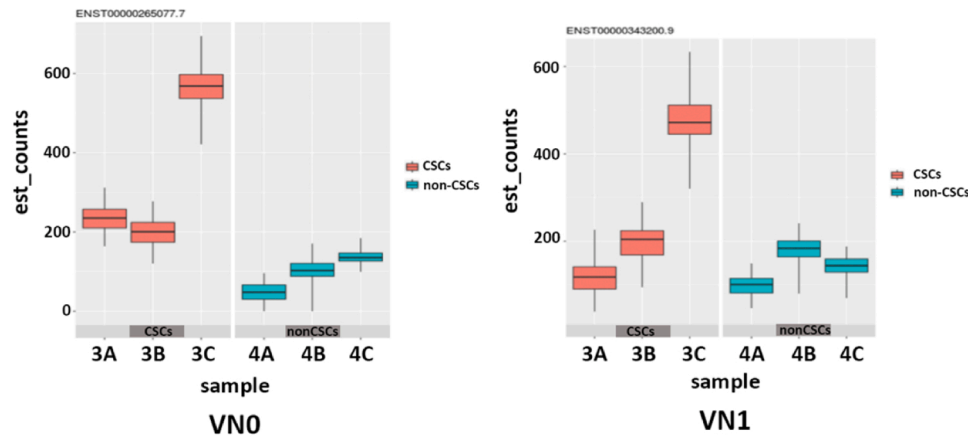| Transcript_id	Isoform	test_stat	P-value	mean_obs	var_obs
ENST00000265077.7	VN0	4,192164	0,04061122	5,096586	0,6922689
ENST00000343200.9	VN1	0,9834842	0,3213401	5,192348	0,2764772
ENST00000342785.8	VN2	not significant			
ENST00000502527.2	VN3	not significant			
ENST00000512590.6	VN4	not significant			

Fig. 6. The comparative analysis of VN0 and VN1 transcripts in CSCs and non-CSCs.
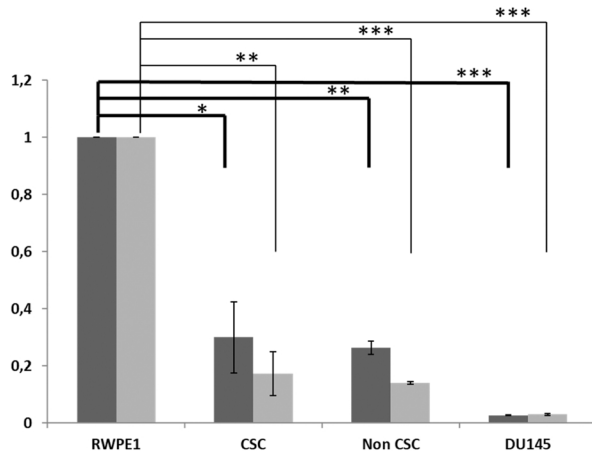

Fig. 7. Comparative qRT-PCR analysis of versican isoforms, V0 and V1. Data are presented as the mean $\pm$ SD from three independent experiments with triple replicates per experiment. p values: *p $\leq$0.05, **P $\leq$ 0.01, and ***P $\leq$ 0.001 indicate a significant difference compared to the prostatic non-cancerous epithelial cells of the RWPE-1 group. CSC: cancer stem cells, Non CSC: non-cancer stem cells.

CRediT authorship contribution statement

Gulperi Oktem: Supervision, Conceptualization. **Aysegul Taskiran:** Methodology, Investigation. **Sercin Karahuseyinoglu:** Writing – original draft. **Ilknur Keskin:** Methodology, Investigation. **Cuneyd Parlayan:** Visualization, Validation. **Yasemin Yozgat Byrne:** Visualization, Validation. **Emre Karakoc:** Visualization, Validation. **Şule Ayla:** Writing – original draft, Supervision, Methodology, Investigation, Conceptualization.

Declaration of Competing Interest

The authors declare that they have no known competing financial interests or personal relationships that could have appeared to influence the work reported in this paper.

Acknowledgments

Not applicable.

Patient consent for publication

Not applicable.

References

[1] G. Rafikova, I. Gilyazova, K. Enikeeva, V. Pavlov, J. Kzhyshkowska, Prostate cancer: genetics, epigenetics and the need for immunological biomarkers, Int. J. Mol. Sci. 24 (2023), https://doi.org/10.3390/ijms241612797.

[2] J.S. Lawson, W.K. Glenn, Multiple pathogens and prostate cancer, Infect. Agent Cancer 17 (2022), https://doi.org/10.1186/s13027-022-00427-1.

[3] C.V. Berenguer, F. Pereira, J.S. Câmara, J.A.M. Pereira, Underlying features of prostate cancer—statistics, risk factors, and emerging methods for its diagnosis, Curr. Oncol. 30 (2023) 2300–2321, https://doi.org/10.3390/curroncol30020178.

[4] T.M. Seibert, I.P. Garraway, A. Plym, B.A. Mahal, V. Giri, M.F. Jacobs, et al., Genetic risk prediction for prostate cancer: implications for early detection and prevention, Eur. Urol. 83 (2023) 241–248, https://doi.org/10.1016/J.EURURO.2022.12.021.

[5] A. Pérez-González, K. Bévant, C. Blanpain, Cancer cell plasticity during tumor progression, metastasis and response to therapy, Nat. Cancer 4 (8) (2023) 1063–1082, https://doi.org/10.1038/s43018-023-00595-y.

[6] Q. Wang, X. Shao, Y. Zhang, M. Zhu, F.X.C. Wang, J. Mu, et al., Role of tumor microenvironment in cancer progression and therapeutic strategy, Cancer Med 12 (2023) 11149–11165, https://doi.org/10.1002/cam4.5698.

[7] A. Taskiran, A. Demir, E. Acikgoz, G. Oktem, Cancer stem cells and nitric oxide, Nitric Oxide Health Dis.: Ther. Appl. Cancer Inflamm. Disord. (2023) 135–150, https://doi.org/10.1016/B978-0-443-13342-8.00019-3.

[8] H. Zhou, L. Tan, B. Liu, X.Y. Guan, Cancer stem cells: recent insights and therapies, Biochem. Pharm. 209 (2023), https://doi.org/10.1016/j.bcp.2023.115441.

[9] X. He, B. Lee, Y. Jiang, Extracellular matrix in cancer progression and therapy, Med. Rev. 2 (2022) 125–139, https://doi.org/10.1515/mr-2021-0028.

[10] S. Nallanthighal, J.P. Heiserman, D.J. Cheon, The role of the extracellular matrix in cancer stemness, Front. Cell Dev. Biol. 7 (2019) 86, https://doi.org/10.3389/FCELL.2019.00086.

[11] D. Wang, Y. Li, H. Ge, T. Ghadban, M. Reeh, C. Güngör, The extracellular matrix: a key accomplice of cancer stem cell migration, metastasis formation, and drug resistance in PDAC, Cancers Vol 14 (2022) 3998, https://doi.org/10.3390/CANCERS14163998.

[12] C. Walker, E. Mojares, A. Del Río Hernández, Role of extracellular matrix in development and cancer progression, Int. J. Mol. Sci. 19 (2018), https://doi.org/10.3390/ijms19103028.

[13] Y.J. Wu, D.P. La Pierre, J. Wu, A.J. Yee, B.B. Yang, The interaction of versican with its binding partners, Cell Res. 15 (7) (2005) 483–494, https://doi.org/10.1038/sj.cr.7290318.

[14] M. Hasan, J. Shovon, D.A. Khan, M. Mohaimenul, I. Tareq, N.H. Zilani, et al., A comprehensive assessment of VCAN transcriptional regulation and evaluation as an effective prognostic biomarker against breast cancer: in silico study, Bull. Natl. Res. Cent. 47 (1) (2023) 1–16, https://doi.org/10.1186/S42269-023-01062-5.

[15] T.N. Wight, M.G. Kinsella, S.P. Evanko, S. Potter-Perigo, M.J. Merrilees, Versican and the regulation of cell phenotype in disease, Biochim. Biophys. Acta Gen. Subj. 1840 (2014) 2441–2451, https://doi.org/10.1016/j.bbagen.2013.12.028.

[16] Wight T.N., Day A.J., Kang I., Harten I.A., Kaber G., Briggs D.C., et al. V3: an enigmatic isoform of the proteoglycan versican. Https://DoiOrg/101152/Ajpcell000592023 2023;325:C519–37. https://doi.org/10.1152/AJPCELL.00059.2023.

[17] K. Matsumoto, M. Shionyu, M. Go, K. Shimizu, T. Shinomura, K. Kimata, et al., Distinct interaction of versican/PG-M with hyaluronan and link protein, J. Biol. Chem. 278 (2003) 41205–41212, https://doi.org/10.1074/JBC.M305060200.

[18] T.N. Wight, Versican: a versatile extracellular matrix proteoglycan in cell biology, Curr. Opin. Cell Biol. 14 (2002) 617–623, https://doi.org/10.1016/S0955-0674(02)00375-7.

[19] Md.H.J. Shovon, D.A. Khan, Md.M.I. Tareq, Md Imtiaz, M.N.H. Zilani, Md. N. Hasan, A comprehensive assessment of VCAN transcriptional expression and evaluation as an effective prognostic biomarker against breast cancer: in silico study, Bull. Natl. Res Cent. (2023) 47, https://doi.org/10.1186/s42269-023-01062-5.

[20] K. Fanhchaksai, F. Okada, N. Nagai, P. Pothacharoen, P. Kongtawelert, S. Hatano, et al., Host stromal versican is essential for cancer-associated fibroblast function to inhibit cancer growth, Int. J. Cancer 138 (2016) 630–641, https://doi.org/10.1002/IJC.29804.

[21] L.F. Brown, A.J. Guidi, S.J. Schnitt, L. Van De Water, M.L. Iruela-Arispe, T.K. Yeo, et al., Vascular stroma formation in carcinoma in situ, invasive carcinoma, and metastatic carcinoma of the breast, Clin. Cancer Res. 5 (1999) 1041–1056.

[22] Z. Isogai, A. Aspberg, D.R. Keene, R.N. Ono, D.P. Reinhardt, L.Y. Sakai, Versican interacts with fibrillin-1 and links extracellular microfibrils to other connective tissue networks, J. Biol. Chem. 277 (2002) 4565–4572, https://doi.org/10.1074/JBC.M110583200.

[23] Ricciardelli Carmela, H.Brooks John, Suwiwat Supaporn, J.Sakko Andrew, Mayne Keiko, A.Raymond Wendy, et al., Regulation of stromal versican expression by breast cancer cells and importance to relapse-free survival in patients with node-negative primary breast cancer, Clin. Cancer Res. (2002) 1054–1960, https://pubmed.ncbi.nlm.nih.gov/11948113/ (accessed October 9, 2023).

[24] M. Serra, L. Miquel, C. Domenzain, M.J. Docampo, A. Fabra, T.N. Wight, et al., V3 versican isoform expression alters the phenotype of melanoma cells and their tumorigenic potential, Int. J. Cancer 114 (2005) 879–886, https://doi.org/10.1002/ijc.20813.

[25] W. Paulus, I. Baur, M.T. Dours-Zimmermann, D.R. Zimmermann, Differential expression of versican isoforms in brain tumors, J. Neuropathol. Exp. Neurol. 55 (1996) 528–533, https://doi.org/10.1097/00005072-199605000-00005.

[26] B.L. Yang, Y. Zhang, L. Cao, B.B. Yang, Cell adhesion and proliferation mediated through the G1 domain of versican, J. Cell Biochem (1999) 210–220, https://pubmed.ncbi.nlm.nih.gov/10022503/ (accessed October 9, 2023).

[27] P.S. Zheng, D. Vais, D. LaPierre, Y.Y. Liang, V. Lee, B.L. Yang, et al., PG-M/versican binds to P-selectin glycoprotein ligand-1 and mediates leukocyte aggregation, J. Cell Sci. 117 (2004) 5887–5895, https://doi.org/10.1242/JCS.01516.

[28] P.S. Zheng, J. Wen, L.C. Ang, W. Sheng, A. Viloria-Petit, Y. Wang, et al., Versican/PG-M G3 domain promotes tumor growth and angiogenesis, FASEB J. 18 (2004) 754–756, https://doi.org/10.1096/FJ.03-0545FJE.

[29] S.P. Evanko, E.W. Raines, R. Ross, L.I. Gold, T.N. Wight, Proteoglycan distribution in lesions of atherosclerosis depends on lesion severity, structural characteristics, and the proximity of platelet-derived growth factor and transforming growth factor-beta, Am. J. Pathol. 152 (1998) 533.

[30] W. Sheng, G. Wang, D.P. La Pierre, J. Wen, Z. Deng, C.-K.A. Wong, et al., Versican mediates mesenchymal-epithelial transition, Mol. Biol. Cell 17 (2006) 2009–2020, https://doi.org/10.1091/mbc.e05-10-0951.

[31] C. Tatar, C.B. Avci, E. Acikgoz, G. Oktem, Doxorubicin-induced senescence promotes resistance to cell death by modulating genes associated with apoptotic and necrotic pathways in prostate cancer DU145 CD133+/CD44+ cells, Biochem Biophys. Res. Commun. (2023), https://doi.org/10.1016/j.bbrc.2023.09.032.

[32] R. Mori, Q. Wang, K.D. Danenberg, J.K. Pinski, P.V. Danenberg, Both β-actin and GAPDH are useful reference genes for normalization of quantitative RT-PCR in human FFPE tissue samples of prostate cancer, Prostate 68 (2008) 1555–1560, https://doi.org/10.1002/PROS.20815.

[33] X.H. Shen, W.R. Lin, M.D. Xu, P. Qi, L. Dong, Q.Y. Zhang, et al., Prognostic significance of Versican expression in gastric adenocarcinoma, Oncogenesis 4 (2015) e178, https://doi.org/10.1038/ONCSIS.2015.36.

[34] N. Yamauchi, Y. Kanke, K. Saito, H. Okayama, S. Yamada, S. Nakajima, et al., Stromal expression of cancer-associated fibroblast-related molecules, versican and lumican, is strongly associated with worse relapse-free and overall survival times in patients with esophageal squamous cell carcinoma, Oncol. Lett. 21 (2021), https://doi.org/10.3892/ol.2021.12706.

[35] K. Kato, M. Fukai, K.C. Hatanaka, A. Takasawa, T. Aoyama, T. Hayasaka, et al., Versican secreted by cancer-associated fibroblasts is a poor prognostic factor in hepatocellular carcinoma, Ann. Surg. Oncol. 29 (2022) 7135–7146, https://doi.org/10.1245/s10434-022-11862-0.

[36] Islam, Watanabe. Core Protein Structure and Variant Forms. n.d.

[37] K. Asano, C.M. Nelson, S. Nandadasa, N. Aramaki-Hattori, D.J. Lindner, T. Alban, et al., Stromal versican regulates tumor growth by promoting angiogenesis, Sci. Rep. 7 (2017), https://doi.org/10.1038/S41598-017-17613-6.

[38] B. Soner, E. Açikgöz, S. Caggia, S. Khan, A. Taşkiran, G. Öktem, Different mRNA and protein expression of versican in TGF-β1-treated prostate cancer cells, Forbes J. Med. 3 (2022) 197–202, https://doi.org/10.4274/forbes.galenos.2022.35229.

[39] J. Guo, Y. Liu, INHBA promotes the proliferation, migration and invasion of colon cancer cells through the upregulation of VCAN, J. Int. Med. Res. 49 (2021), https://doi.org/10.1177/03000605211014998.

[40] Q. Zhang, J. Wu, X. Chen, M. Zhao, D. Zhang, F. Gao, Upregulation of versican associated with tumor progression, metastasis, and poor prognosis in bladder carcinoma, Biomed. Res. Int. 2021 (2021), https://doi.org/10.1155/2021/6949864.

[41] G. Sun, W. Zheng, P. Tan, J. Zhou, W. Tang, H. Cao, et al., Comprehensive analysis of VCAN expression profiles and prognostic values in HCC, Front. Genet. 13 (2022) 1, https://doi.org/10.3389/FGENE.2022.900306/FULL.

[42] W. Chang, J. Zhu, D. Yang, A. Shang, Z. Sun, W. Quan, et al., Plasma versican and plasma exosomal versican as potential diagnostic markers for non-small cell lung cancer, Respir. Res. 24 (2023), https://doi.org/10.1186/S12931-023-02423-4.

[43] L. Zhai, W. Chen, B. Cui, B. Yu, Y. Wang, H. Liu, Overexpressed versican promoted cell multiplication, migration and invasion in gastric cancer, Tissue Cell 73 (2021) 101611, https://doi.org/10.1016/J.TICE.2021.101611.

[44] W. Li, F. Han, M. Fu, Z. Wang, High expression of VCAN is an independent predictor of poor prognosis in gastric cancer, J. Int. Med. Res. 48 (1) (2020) 11, https://doi.org/10.1177/0300060519891271.

[45] H. Gao, Y. Cheng, Y. Chen, F. Luo, Y. Shao, Z. Sun, et al., The expression of versican and its role in pancreatic neuroendocrine tumors, Pancreatology 20 (2020) 142–147, https://doi.org/10.1016/j.pan.2019.11.009.

[46] Y. Cheng, H. Sun, L. Wu, F. Wu, W. Tang, X. Wang, et al., Vup-regulation of vcan promotes the proliferation, invasion and migration and serves as a biomarker in gastric cancer, Onco Targets Ther. 13 (2020) 8665–8675, https://doi.org/10.2147/OTT.S262613.

[47] X. yan Huang, J. jian Liu, X. Liu, Y. hui Wang, W. Xiang, Bioinformatics analysis of the prognosis and biological significance of VCAN in gastric cancer, Immun. Inflamm. Dis. 9 (2021) 547–559, https://doi.org/10.1002/iid3.414.

[48] L. Zhang, J. Bi, X. Yu, X. Li, X. Liu, X. Weng, et al., Versican core protein aids in the diagnosis and grading of breast phyllodes tumor, Ann. Diagn. Pathol. 66 (2023), https://doi.org/10.1016/j.anndiagpath.2023.152176.

[49] H.L. Luo, Y.L. Chang, H.Y. Liu, Y.T. Wu, M.T. Sung, Y.L. Su, et al., VCAN hypomethylation and expression as predictive biomarkers of drug sensitivity in upper urinary tract urothelial carcinoma, Int J. Mol. Sci. 24 (2023), https://doi.org/10.3390/ijms24087486.

[50] A.V. Suhovskih, L.A. Mostovich, I.S. Kunin, M.M. Boboev, G.I. Nepomnyashchikh, S.V. Aidagulova, et al., Proteoglycan expression in normal human prostate tissue and prostate cancer, ISRN Oncol. 2013 (2013) 1–9, https://doi.org/10.1155/2013/680136.

[51] N.A. Cross, S. Chandrasekharan, N. Jokonya, A. Fowles, F.C. Hamdy, D.J. Buttle, et al., The expression and regulation of ADAMTS-1, -4, -5, -9, and -15, and TIMP-3 by TGFbeta1 in prostate cells: relevance to the accumulation of versican, Prostate 63 (2005) 269–275, https://doi.org/10.1002/PROS.20182.

[52] G. Oktem, O. Sercan, U. Guven, R. Uslu, A. Uysal, G. Goksel, et al., Cancer stem cell differentiation: TGFβ1 and versican may trigger molecules for the organization of tumor spheroids, Oncol. Rep. 32 (2014) 641–649, https://doi.org/10.3892/OR.2014.3252/HTML.

[53] M. Marzagalli, F. Fontana, M. Raimondi, P. Limonta, Cancer stem cells-key players in tumor relapse, Cancers (Basel) 13 (2021) 1–23, https://doi.org/10.3390/CANCERS13030376.